JPP
Journal of
Pharmacy and Pharmacology

JPP 2009, 61: 631–640

Received November 21, 2008
Accepted February 4, 2009
DOI 10.1211/jpp/61.05.0012
ISSN 0022-3573

Research Paper

Pharmacological and metabolic characterisation of the potent σ_1 receptor ligand 1′-benzyl-3-methoxy-3*H*-spiro[[2]benzofuran-1,4′-piperidine]

Christian Wiese[a], Eva Große Maestrup[a], Dirk Schepmann[a], Jose Miguel Vela[b], Jörg Holenz[b], Helmut Buschmann[b] and Bernhard Wünsch[a]

[a]Institut für Pharmazeutische und Medizinische Chemie der Universität Münster, Münster, Germany and [b]Esteve, Barcelona, Spain

Abstract

Objectives The pharmacology and metabolism of the potent σ_1 receptor ligand 1′-benzyl-3-methoxy-3*H*-spiro[[2]benzofuran-1,4′-piperidine] were evaluated.

Methods The compound was tested against a wide range of receptors, ion channels and neurotransmitter transporters in radioligand binding assays. Analgesic activity was evaluated using the capsaicin pain model. Metabolism by rat and human liver microsomes was investigated, and the metabolites were identified by a variety of analytical techniques.

Key findings 1′-Benzyl-3-methoxy-3*H*-spiro[[2]benzofuran-1,4′-piperidine] (compound **1**) is a potent σ_1 receptor ligand (K_i 1.14 nM) with extraordinarily high σ_1/σ_2 selectivity (>1100). It was selective for the σ_1 receptor over more than 60 other receptors, ion channels and neurotransmitter transporters, and did not interact with the human ether-a-go-go-related gene (hERG) cardiac potassium channel. Compound **1** displayed analgesic activity against neuropathic pain in the capsaicin pain model (53% analgesia at 16 mg/kg), indicating that it is a σ_1 receptor antagonist. It was rapidly metabolised by rat liver microsomes. Seven metabolites were unequivocally identified; an N-debenzylated metabolite and a hydroxylated metabolite were the major products. Pooled human liver microsomes formed the same metabolites. Studies with seven recombinant cytochrome P450 isoenzymes revealed that CYP3A4 produced all the metabolites identified**.** The isoenzyme CYP2D6 was inhibited by **1** (IC50 88 nM) but did not produce any metabolites.

Conclusions 1′-Benzyl-3-methoxy-3*H*-spiro[[2]benzofuran-1,4′-piperidine] is a potent and selective σ_1 receptor antagonist, which is rapidly metabolised. Metabolically more stable σ_1 ligands could be achieved by stabilising the N-benzyl substructure.

Keywords analgesic activity; metabolism; σ_1 receptor antagonists; recombinant CYP isoenzymes; spirocyclic piperidines

Introduction

When the σ receptor was discovered it was classified as an opioid receptor subtype, because typical opioid receptor ligands of the benzomorphan type produced atypical pharmacological effects.[1] However, further investigations revealed that most of the effects caused by typical σ ligands were not antagonised by the opioid receptor antagonist naloxone and so this classification was discarded.[2] The next hypothesis – that the σ receptor and the phencyclidine (PCP) binding site of the *N*-methyl-D-aspartate (NMDA) receptor are identical – was also disproved, because the antipsychotic agent haloperidol binds with high affinity to σ receptors but has no affinity for the PCP binding site.[3] Sigma receptors are now well established as a non-opioid, non-PCP and haloperidol-sensitive receptor family with their own binding profile and a characteristic distribution in the central nervous system (CNS) as well as in endocrine, immune and some peripheral tissues such as the kidney, liver, lung and heart.[4,5]

Today, at least two σ receptor subtypes have been identified, which are termed σ_1 and σ_2 receptors. Both subtypes bind haloperidol and di-*o*-tolylguanidine with high affinity. However, they differ in their interaction with dextrorotatory benzomorphans: whereas the

Correspondence:
Bernhard Wünsch, Institut für Pharmazeutische und Medizinische Chemie der Universität Münster, Hittorfstraße 58–62, D-48149 Münster, Germany.
E-mail: wuensch@uni-muenster.de

σ_1 subtype displays high affinity for (+)-benzomorphans (e.g. (+)-pentazocine and (+)-SKF-10,047), the σ_2 subtype shows only low affinity for these benzomorphan enantiomers.[6]

About 10 years ago the σ_1 receptor was cloned from various tissues and species, including guinea-pig liver,[7] rat brain[8] and human placental choriocarcinoma cell lines.[9] Whereas the similarity between σ_1 receptors from various species is very high (>92% identity, >95% similarity), there is no significant homology with any other known mammalian protein. However, the yeast enzyme ergosterol-Δ^8/Δ^7-isomerase shows approximately 30% homology with the σ_1 receptor. The rat brain σ_1 gene encodes for a protein consisting of 223 amino acids with a molecular weight of 23 kDa. A model of the membrane-bound σ_1 receptor was proposed in 2002, showing two transmembrane domains with both the C- and N-termini localised intracellularly.[10]

The molecular weight of the σ_2 receptor (21.5 kDa), which has not been cloned so far, is less than that of the σ_1 receptor.[11] Endogenous ligands for the σ_1 and σ_2 receptor have yet to be identified, but studies have revealed that neuro (active) steroids such as pregnenolone, progesterone and dehydroepiandrosterone interact with moderate affinity with the σ_1 receptor and are therefore proposed to be its endogenous ligands.[12]

It has been shown that σ_1 receptors are involved in the modulation of various neurotransmitter systems, including glutamatergic,[13] dopaminergic[14] and cholinergic[15] neurotransmission. Another important feature of σ_1 receptors is their influence on the regulation and activity of potassium channels[16,17] and calcium channels.[18,19] Ligands that interact with σ_1 receptors may therefore have potential in the treatment of acute and chronic neurological disorders, including schizophrenia,[20] depression,[21,22] Alzheimer's disease and Parkinson's disease,[23,24] as well as alcohol and cocaine abuse.[25,26] Moreover, σ_1 receptor ligands have analgesic potential. In particular, σ_1 receptor antagonists are useful for the treatment of neuropathic pain.[27,28] It has been demonstrated that σ_1 receptor antagonists such as BD1047, BD1063 (1-[2-(3,4-dichlorophenyl)ethyl]-4-methylpiperazine dihydrochloride) and NE100 produce analgesic effects in formalin- or capsaicin-induced pain models. The contribution of σ_1 receptors has been shown using σ_1 receptor knockout mice.[29–31]

Investigations of brain σ_1 receptors using positron emission tomography (PET) and single-photon emission computed tomography (SPECT) may provide significant contributions to understanding of the cross talk between σ_1 receptors and brain neurotransmitter systems. The new insights into these functional interrelationships could improve the diagnosis of several brain diseases and the development of new therapeutic concepts. Radiotracers for PET or SPECT studies that are suitable for clinical application are not currently available, however.

We have previously reported on the synthesis and receptor binding studies of a new class of spirocyclic piperidines that bind with high affinity to σ_1 receptors.[32,33] Based on these compounds, we plan to develop PET and SPECT tracers suitable for clinical use that would enable analysis of the distribution and activity of σ_1 receptors in the CNS.

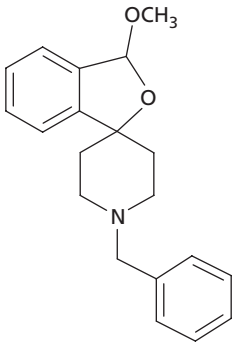

Figure 1 Spirocyclic compound **1** with high σ_1 receptor affinity.

1′-Benzyl-3-methoxy-3H-spiro[[2]benzofuran-1,4′-piperidine] (compound **1**; Figure 1) was selected on the basis of its high affinity towards σ_1 receptors (K_i value 1.14 nM).[32] Here we report on the pharmacological evaluation of this compound and its metabolism. Metabolic stability is a major requirement for PET tracers because degradation products could compromise the validity of experiments. Knowledge of the metabolic stability and the metabolism pathways of the compounds can help in the development of new compounds with better metabolic stability.

Materials and Methods

Receptor selectivity

The affinity of compound **1** towards the following receptors was investigated (the radioligand used in the assay is given in parentheses): adenosine A_1 receptor (1 nM [^{3}H] DPCPX); adenosine A_{2A} (0.05 μM [^{3}H] CGS-21680); adenosine A_3 (0.5 nM [^{125}I] AB-MECA); α_{1A} adrenoceptor (0.25 nM [^{3}H] prazosin); α_{1B} adrenoceptor (0.25 nM [^{3}H] prazosin); α_{1D} adrenoceptor (0.6 nM [^{3}H] prazosin); α_{2A} adrenoceptor (1 nM [^{3}H] MK-912); β_1 adrenoceptor (0.03 nM [^{125}I] cyanopindolol); β_2 adrenoceptor (0.2 nM [^{3}H] CGP-12177); bradykinin B_1 (0.5 nM [^{3}H] (Des-Arg^{10})-kallidin); bradykinin B_2 (0.2 nM [^{3}H] bradykinin); dopamine D_1 (1.4 nM [^{3}H] SCH-23390); dopamine D_2 (0.16 nM [^{3}H] spiperone); dopamine D_3 (0.7 nM [^{3}H] spiperone); dopamine $D_{4.2}$ (0.5 nM [^{3}H] spiperone); endothelin ET_A (0.03 nM [^{125}I] endothelin-1); endothelin ET_B (0.1 nM [^{125}I] endothelin-1); epidermal growth factor (EGF) (0.05 nM [^{125}I] murine EGF); estrogen ERα (0.5 nM [^{3}H] estradiol); $GABA_A$, agonist site (1 nM [^{3}H] muscimol); $GABA_A$, benzodiazepine, central (1 nM [^{3}H] flunitrazepam); gamma aminobutyric acid $(GABA)_B$, non-selective (0.6 nM [^{3}H] CGP-54626); glucocorticoid (6 nM [^{3}H] dexamethasone); glutamate, kainate (5 nM [^{3}H] kainic acid); glutamate, NMDA, agonist (2 nM [^{3}H] CGP-39653); glutamate, NMDA, glycine (0.33 nM [^{3}H] MDL-105519); glutamate, NMDA, PCP (4 nM [^{3}H] TCP); histamine H_1 (1.2 nM [^{3}H] pyrilamine); histamine H_2 (0.1 nM [^{125}I] aminopotentidine); histamine H_3 (3 nM [^{3}H] R(−)-α-methylhistamine (RAMH)); imidazoline I_2, central (2 nM [^{3}H] idazoxan); interleukin (IL)-1 (10 pM [^{125}I] IL-1α); leukotriene, cysteinyl $cysLT_1$ (0.3 nM [^{3}H] leukotriene D_4); muscarinic M_1 (0.29 nM [^{3}H] *N*-methylscopolamine); muscarinic M_2

(0.29 nM [^{3}H] *N*-methylscopolamine); muscarinic M_3 (0.29 nM [^{3}H] *N*-methylscopolamine); neuropeptide Y_1 (0.013 nM [^{125}I] peptide YY); neuropeptide Y_2 (20 pM [^{125}I] peptide YY); nicotinic (0.1 nM [^{125}I] epibatidine); opioid δ (OP1, DOP) (0.9 nM [^{3}H] naltrindole); opioid κ (OP2, KOP) (0.6 nM [^{3}H] diprenorphine); opioid μ (OP3, MOP) (0.6 nM [^{3}H] diprenorphine); phorbol ester (3 nM [^{3}H] PDBu); platelet activating factor (PAF) (0.12 nM [^{3}H] PAF); purinergic P_{2x} (8 nM [^{3}H] α, β-methylene-ATP); purinergic P_{2Y} (0.1 nM [^{35}S] ATP-α-S); serotonin (5-hydroxytryptamine) 5-HT_{1A} (1.5 nM [^{3}H] 8-OH-DPAT); serotonin 5-HT_3 (0.69 nM [^{3}H] GR-65630); σ_1 (8 nM [^{3}H] haloperidol); σ_2 (3 nM [^{3}H] ifenprodil); tachykinin NK_1 (0.25 nM [^{3}H] SR-140333); testosterone (1.5 nM [^{3}H] mibolerone).

The affinity of compound **1** towards the following ion channels was investigated (the radioligand employed in the assay is given in parentheses): calcium channel benzothiazepine L-type (2 nM [^{3}H] diltiazem); calcium channel dihydropyridine L-type (0.1 nM [^{3}H] nitrendipine); calcium channel N-type (10 pM [^{125}I]ω-conotoxin GVIA); potassium channel [K_{ATP}] (5 nM [^{3}H] glyburide); human ether-a-go-go-related gene (hERG) potassium channel HERG (1.5 nM [^{3}H] astemizole); sodium channel site 2 (5 nM [^{3}H] batrachotoxin).

The affinity of compound **1** towards the following transporters was also investigated (the radioligand used in the assay is given in parentheses): dopamine (DAT) (0.15 nM [^{125}I] RTI-55); GABA (6 nM [^{3}H] GABA); noradrenaline (NET) (0.2 nM [^{125}I] RTI-55); serotonin (5-HT) (SERT) (0.15 nM [^{125}I] RTI-55).

Interaction with the hERG channel

The effects of compound **1** on hERG potassium channel activity were investigated using a fluorescence assay and was performed by Evotec AG (Hamburg, Germany). The fluorescence-based microplate assay was performed using Chinese hamster ovary (CHO)-cells stably transfected with the hERG potassium channel, and wild-type CHO cells as control. The assay is based on the observation that inhibition of potassium channel activity causes a positive shift in membrane potential, which can be measured using potentiometric dyes.[34–36] Fluorescence was measured with a Tecan Safire-fluorescence reader (Tecan, Crailsheim, Germany) on 384-well plates.

Compound **1** was tested at 10 μM and the mean fluorescence increase was correlated to remaining hERG channel activity. Full block of hERG-channel-mediated activity in the cell-based assay results in a remaining activity of 0, whereas if compounds have no effect on the ion channel-mediated activity the remaining activity is about 1.0.

Capsaicin assay

Animals

Male CD1 mice (Harlan Ibérica, Barcelona, Spain), aged 6–8 weeks were used. Animals were housed in groups of five and provided with food and water *ad libitum* and kept in controlled laboratory conditions (temperature 21 ± 1°C and light in 12 h cycles (on at 07:00 h and off at 19:00 h)). Experiments were carried out in a soundproof and air-regulated room. The number of mice in each individual experiment ranged from 8 to 16 per group. All experimental procedures and animal husbandry were conducted according to ethical principles for the evaluation of pain in conscious animals and to ethical guidelines of the European Community on the Care and Use of Laboratory Animals (European Communities Council Directive of 24 November 1986, 86/609/ECC) and received approval by the local ethical committee.

Drugs

Capsaicin (8-methyl-N-vanillylnon-6-enamide) was purchased from Sigma (St Louis, MO, USA) and dissolved in 1% DMSO (vehicle). Drugs used for treatments were dissolved in 1% DMSO. All compounds and vehicles were administered in a volume of 5 ml/kg body weight via the subcutaneous route.

Mice were injected with capsaicin (1 μg in 20 μl 1% DMSO) or 1% DMSO (vehicle) into the mid-plantar surface of the right hind paw. The σ_1 ligand was administered 30 min before capsaicin injection. Withdrawal latency to a mechanical stimulus was determined 15 min after capsaicin injection.

Evaluation of mechanical allodynia: von Frey test

Mechanical allodynia was quantified by measuring the hind-paw withdrawal response latency to von Frey filament stimulation. Mice were placed in compartment enclosures in a test chamber with a framed metal mesh floor and allowed to acclimatise to their environment for 2 h before testing. The mechanical stimulus was applied to the plantar surface of the right capsaicin-injected hind paw from below the mesh floor, using an automated testing device (dynamic plantar aesthesiometer; Ugo Basile, Comerio, Italy). The device raises a straight filament (0.5 mm diameter) that exerts a fixed upward pressure (1 g) on the plantar surface. The mechanical stimulus automatically stops when the animal withdraws its hind paw, and the latency time is recorded. Latency was defined as the time from the onset of exposure to the filament to the cessation of the pressure when the sensor detected the withdrawal of the paw. A cut-off latency of 60 s was imposed. Paw withdrawal latencies were measured in triplicate for each animal. Data are presented as latency time or a percentage of analgesia (antiallodynic effect). When fixed at 1 g, the pressure exerted by the filament is insufficient to induce pain responses in normal control mice (in the absence of capsaicin); thus prompt withdrawal responses found 15 min after sensitisation with 1 μg capsaicin reflect mechanical allodynia. This approach enabled us to evaluate the possible antiallodynic effect of σ_1 ligands.

Statistical methods

Statistical analysis of the analgesic effect on mice was performed using one-way analysis of variance followed by the Newmann–Keul test. A P value below 0.05 was considered statistically significant.

Metabolism studies

Preparation of rat liver microsomes

Rat liver microsomes were prepared according to the method of Dayer and colleagues.[37] Frozen rat livers from male Wistar rats were thawed in phosphate buffer (pH 7.4) with 0.25 M sucrose and 5 mM EDTA, cut into small pieces and homogenised at 4°C (Elvehjem Potter, B. Braun Biotech International; Melsungen, Germany). The resulting suspension was centrifuged at 10 000*g* for 15 min at 4°C (high-speed cooling centrifuge, Sorvall RC-5C plus, Thermo Finnigan (Bremen, Germany). Fat was removed by cellulose. The pellet was resuspended in buffer, and the mixture centrifuged again; the two supernatants were then combined. This suspension was then centrifuged for 60 min at 100 000*g* at 4°C (Beckmann L8-M ultracentrifuge fitted with Ti 70.1 rotor; Beckman, Fullerton, CA, USA). The resulting supernatant (cytosol) was discarded, the pellet carefully washed with buffer, resuspended and the centrifugation repeated at the same speed for 60 min. Finally, the supernatant was removed and the pellet resuspended in a small amount of phosphate buffer (pH 7.4). The microsome suspensions were stored at –80°C.

Incubation with rat liver microsomes

Generally the enzymes in rat liver microsomes are more active than those in human microsomes and preliminary experiments with rat liver microsomes showed that incubations at 20°C and at 37°C gave the same results. Incubations were carried out in phosphate buffer (pH 7.4) at room temperature in a circular shaker (IKA Vibrax VXR, Staufen, Germany) and contained rat liver microsomes (1.5 mg protein/ml), 0.86 mM $MgCl_2$ and 2.6 mM NADPH. The concentration of compound **1** was 260 μM, in a final volume of 0.9 ml. Incubations were stopped after 90 min by addition of ice-cold acetonitrile. The samples were kept at –20°C for 30 min to complete protein precipitation. After thawing, the samples were centrifuged at 10 000*g* for 10 min, then the supernatant was decanted, filtered with a 0.45 μm (pore size) syringe filter made from regenerated cellulose (Macherey-Nagel, Düren, Germany) and analysed.

Seven incubations of compound **1** were carried out as described above, but with a concentration of compound **1** of 320 μM in a total volume of 0.9 ml. For the first hour one incubation was stopped every 10 min by addition of ice cold acetonitrile. Then 145 μl 0.6 mg/ml haloperidol solution was added as internal standard, resulting in a final concentration of 220 μM in the total volume of 1.045 ml. The last incubation was stopped and analysed after 90 min. Calibration was carried out with the same matrix but without NADPH. All calibration standards were handled in the same way as the test samples.

Incubation with human liver microsomes

Pooled human liver microsomes (from Cytonet, Weinheim, Germany) were kindly provided by Bayer HealthCare (Wuppertal, Germany). Compound **1** (20 μM) was incubated for 60 min at 37°C with 0.5 mg protein/ml microsomes in phosphate buffer (pH 7.4) and an NADPH regenerating system consisting of glucose-6-phosphate, NADPH and glucose-6-phosphate dehydrogenase (from *Leuconostoc mesenteroides*). The final NADPH concentration was 1 mM. The incubations were stopped by addition of ice-cold acetonitrile, cooled on ice for 30 min, centrifuged, filtered and analysed as described above.

Studies with recombinant isoenzymes

Cytochrome P450 (CYP) isoenzymes 1A2, 2B6, 2C8, 2C9, 2C19, 2D6 and 3A4 (human P450 BD Gentest Supersomes) were purchased from BD Bioscience (San Jose, CA, USA). Incubations were performed as described for the incubation with the pooled human microsomes, using an enzyme concentration of 0.05 μM.

Oxidation of compound 1 with rat liver microsomes and hydrogen peroxide

In an Erlenmeyer flask on a magnetic stirrer the spirocyclic σ_1 ligand **1** was added to a solution of rat liver microsomes (30 ml, 5 mg protein/ml) in phosphate buffer (pH 7.4) at 37°C. The final concentration of **1** was 0.65 mM in a total volume of 100 ml. Hydrogen peroxide (30%) was added slowly (because of intense foam formation) up to a 'theoretical' concentration of 1.8 M. After 90 min the precipitated proteins were centrifuged (10 000*g*) and CH_2Cl_2 and Na_2SO_4 were added to the supernatant. The organic layer was concentrated *in vacuo* and the residue dissolved in acetonitrile. The mixture was filtered with a syringe filter before purification by preparative HPLC.

Preparative HPLC

Separation was carried out using a Merck Hitachi (Tokyo, Japan) system consisting of a UV detector (L-7400), autosampler (L-7200), pump (L-7150) and interface (D-7000). The column was a Gemini C_{18} 110 Å column (5 μm, 250 × 21.2 mm; Phenomenex, Torrance, CA, USA). The mobile phase, at a flow rate of 15 ml/min, was composed of (A) 100% water and (B) 100% acetonitrile (both containing 0.05% trifluoroacetic acid) using the following gradient: 0 min, 90% A; 18.5 min, 40% A; 19 min, 0% A; 20 min, 0% A; 22 min, 90% A; 25 min, 90% A. In order to isolate the desired compound, the solvent mixture was neutralised with ammonia (25%) to prevent decomposition of the metabolites. Acetonitrile was removed by evaporation *in vacuo* and the water layer was extracted with CH_2Cl_2. The CH_2Cl_2 layer was dried (Na_2SO_4) and concentrated *in vacuo*. The resulting diastereomers were separated by a second preparative HPLC method using the column described above and mobile phase comprising 68.6% acetonitrile, 29.4% water and 2% ammonia (25%), at a flow rate of 15 ml/min.

Analytical HPLC

The same Merck Hitachi equipment was used for analytical purposes. A 20 μl sample of the prepared incubation solution was injected onto a Phenomenex Gemini C_{18} column (5 μm, 250 × 4.6 mm). UV detection was at 210 nm. The mobile phase, at a flow rate of 1.0 ml/min, was composed of (A) 15% acetonitrile in water and (B) 60% acetonitrile in water (both containing 0.05% trifluoroacetic acid) using the following gradient: 0 min, 100% A; 20 min, 0% A;

23 min, 0% A; 24 min, 100% A; 30 min, 100% A. Incubation with rat liver microsomes without NADPH/H^+ led to the identification of the parent compound **1** in the complex matrix (Figure 2).

LC–MS

The HPLC-UV method was transferred to an HPLC system consisting of a Waters Alliance 2690 separation module (Waters, Milford, NE, USA), a Waters 2487 dual λ absorbance detector and a Thermo Finnigan LCQ ion trap mass spectrometer with an electrospray ionisation interface. The ion spray voltage was 3 kV in positive mode, at a sheath gas flow of 80 arbitrary units. The temperature of the capillary was set to 200°C and the capillary voltage to 4 V. A 20 μl volume of the prepared incubation solution was injected onto a LiChrospher RP Select B (250 × 4 mm) column (Merck, Darmstadt, Germany) at a flow rate of 1.0 ml/min. Solvents and gradient were identical to those for the analytical HPLC method. In addition to the MS spectra, UV absorption was recorded at 210 nm.

^{1}H NMR spectrum of metabolite 3

Varian Unity plus 600 MHz. ^{1}H NMR ($CDCl_3$): δ (ppm) = 1.52–1.55 (m, 1H, $N(CH_2CH_2)_2$), 1.72–1.75 (m, 1H, $N(CH_2CH_2)_2$), 2.88–3.0 (m, 2H, $N(CH_2CH_2)_2$), 3.22–3.25 (m broad, 2H, $N(CH_2CH_2)_2$), 3.39 (s, 3H, OCH_3), 3.57–3.64 (m, 2H, $N(CH_2CH_2)_2$), 4.47 (s, 2H, NCH_2Ph), 6.05 (s, 1H, ArCH), 7.18–7.43 (m, 8H, aromat. H), 7.56–7.43 (m, 1H, aromat. H). In order to prove the signals for the piperidine ring protons a ^{1}H TOCSY experiment was carried out.

Results

Receptor selectivity

The spirocyclic piperidine **1** is a very potent σ_1 ligand, showing high selectivity against the σ_2 subtype (1130 fold). At a concentration of 1 μM it did not react with more than 60 other receptors, ion channels and neurotransmitter transporters. In addition to the broad screening, the affinity of the spiropiperidine **1** for 5-HT_6 and 5-HT_7 receptors was investigated. Only very low displacement of the radioligands was observed at a test concentration of 0.1 μM.

Reaction with the hERG channel

CHO cells stably transfected with the hERG channel were used in the assay. The spiropiperidine **1** had little effect on the fluorescence intensity in this assay: about 92% of the hERG channel activity remained after incubation with a concentration of 10 μM of test compound **1**. Compared with the prototypical hERG channel blocker E-4031 (*N*-(4-{1-[2-(6-methylpyridin-2-yl)ethyl]piperidin-4-ylcarbonyl}phenyl)-methanesulfonamide dihydrochloride), which had an IC50 value of 12.3 nM in this assay, the hERG channel blocking activity of **1** is negligible.

Analgesic activity

The antiallodynic effect of the spirocyclic σ_1 ligand **1** was investigated in the capsaicin assay. In this assay, mice were sensitised by subplantar capsaicin injection. Mice were treated with the σ_1 ligand **1** 30 min before capsaicin injection and the withdrawal latency to a mechanical stimulus was determined 15 min after capsaicin injection. The spirocyclic piperidine compound **1** led to 53 ± 6.5% analgesia at a dose of 16 mg/kg and 88 ± 7.0% analgesia at 32 mg/kg.

Metabolism

Rat liver microsomes extensively metabolised compound **1** (Figure 3): after 30 min only 32% of the parent compound remained, and only 10% remained after 60 min. These data indicate rapid metabolic degradation of **1**.

An HPLC separation method was used to separate the formed metabolites (Figure 4) and HPLC–MS equipped with a linear ion trap was used to obtain structural information about the metabolites (Figure 5). MS^n experiments combined with spiking of the samples with reference compounds[32,33]

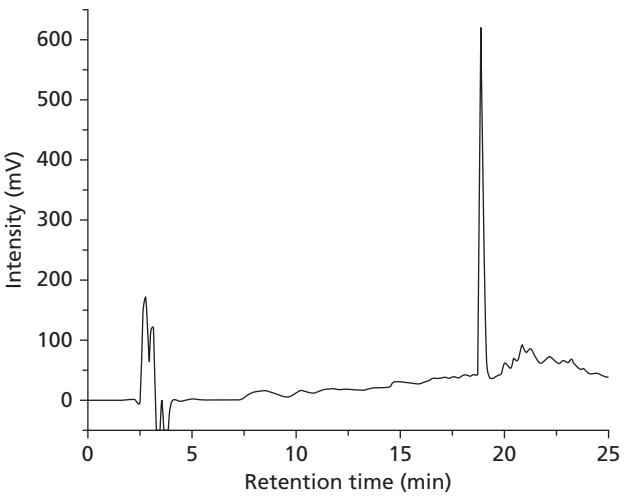

Figure 2 HPLC chromatogram following incubation of compound **1** with rat liver microsomes without NADPH/H^+.

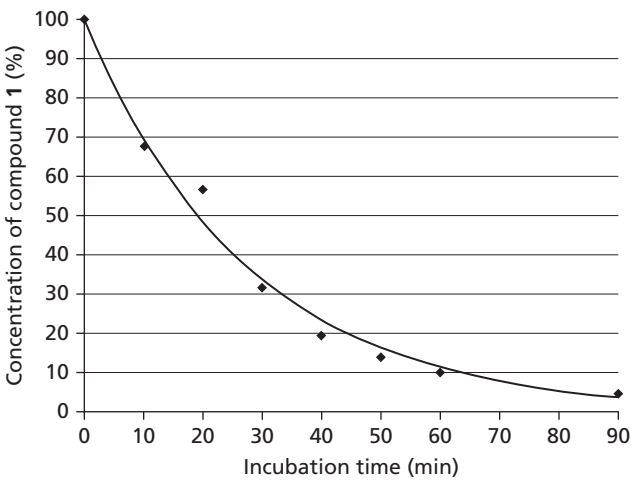

Figure 3 Degradation of spirocyclic compound **1** during incubation with rat liver microsomes.

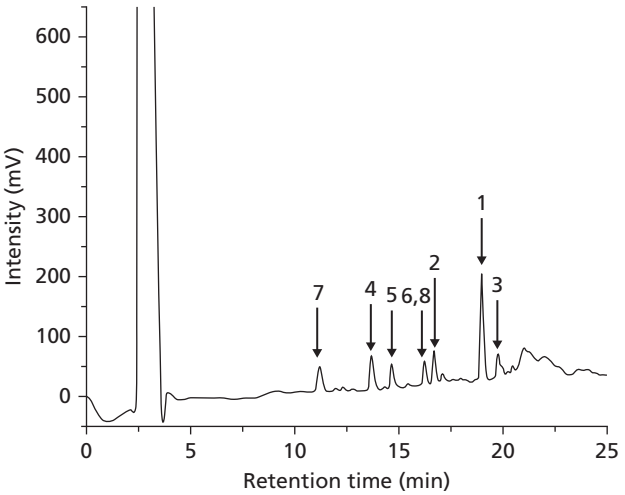

Figure 4 HPLC chromatogram after incubation of **1** with rat liver microsomes and NADPH/H^+.

of potential metabolites led to the identification of seven metabolites **2**–**8**, which are marked on the chromatograms. The structures of the identified metabolites are shown in Figure 6.

The metabolism of **1** was also investigated using pooled human liver microsomes. The metabolic profile was similar to that obtained with rat liver microsomes but markedly less N-oxide **3** was formed, and the second N-oxide **6** was not detected.

In order to elucidate which CYP enzymes are responsible for the fast degradation, the spirocyclic piperidine **1** was incubated with seven important recombinant CYP isoenzymes: 1A2, 2B6, 2C8, 2C9, 2C19, 2D6 and 3A4, and the metabolites formed were analysed using the established HPLC method. CYP3A4 produced all the identified metabolites, particularly the secondary amine **4** and the lactone **8**. Most of the physiologically relevant isoenzymes – CYP2B6, CYP2C8, CYP2C19 and CYP3A4 – led to the formation of the hemiacetal **5**. The isoenzyme CYP2C19 was predominantly responsible for the hydroxylation of the N-benzyl moiety, yielding the hydroxybenzyl metabolite **2**. CYP2D6 did not produce metabolites to a large extent but the spirocyclic piperidine **1** showed a high affinity for this enzyme (IC50 88 nM), indicating that it is a potent inhibitor of this isoenzyme.

Discussion

Receptor selectivity

The selectivity of compound **1** for the σ_1 receptor relative to the σ_2 receptor is of particular interest. In receptor binding studies with the radioligand [^{3}H]-di-*o*-tolylguanidine, a K_i value of 1280 nM (σ_2) was determined, indicating a σ_1/σ_2 selectivity of 1130.[32]

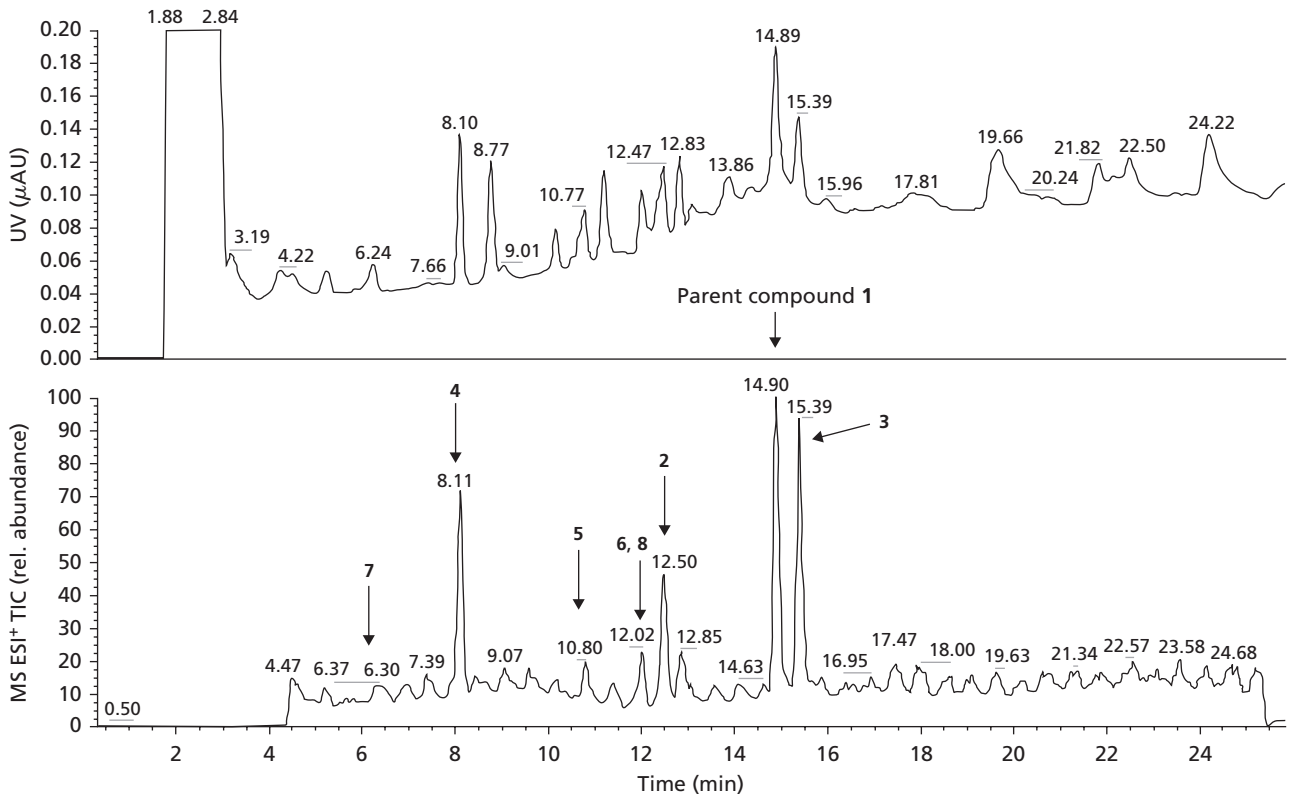

Figure 5 Correlation of HPLC chromatograms with UV (top) and electron spray ionisation (ESI^+)–MS detection (bottom). UV absorption at 210 nm was recorded first, then the solvent was transferred to the ESI–MS. The total ion current (TIC) is displayed.

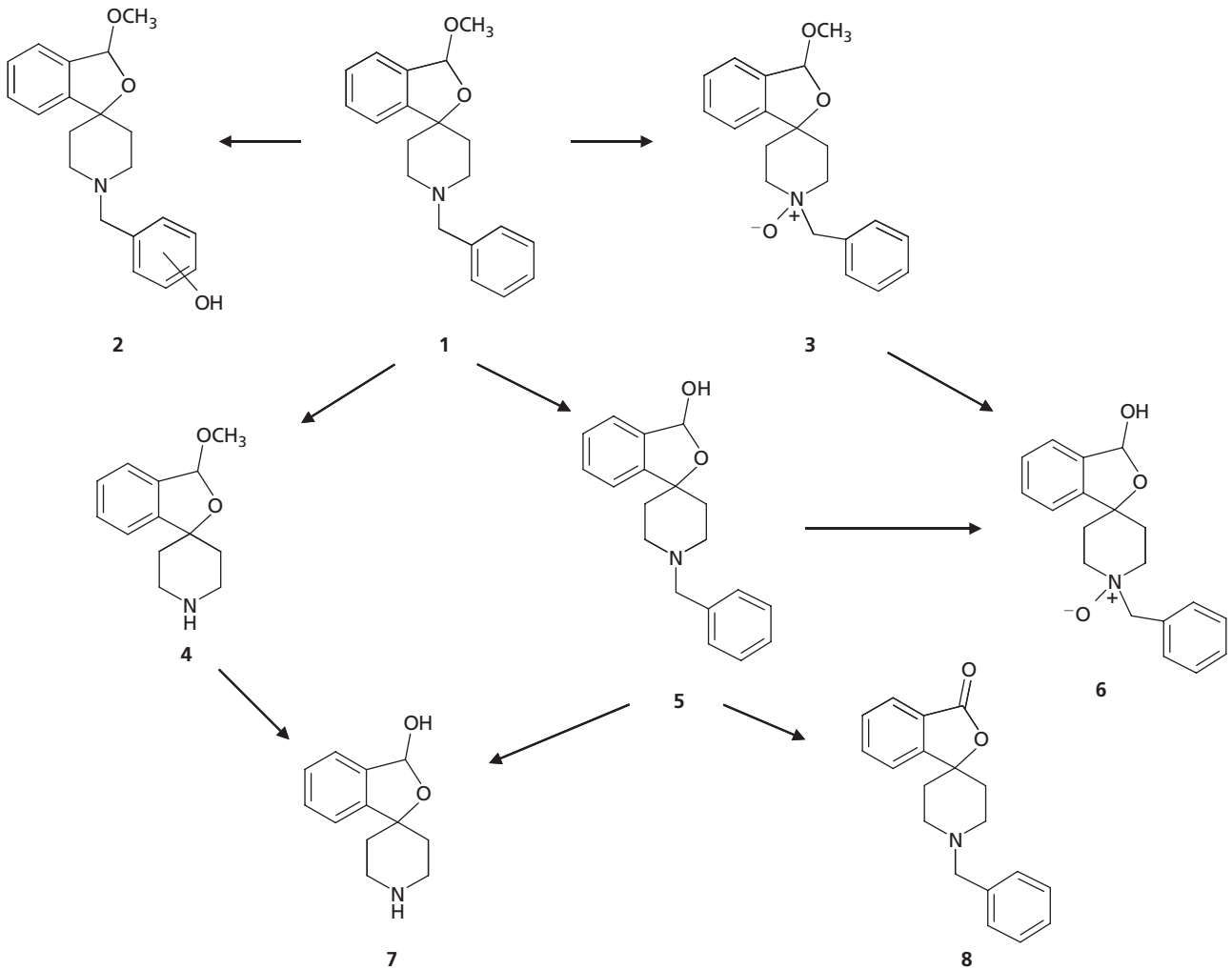

Figure 6 Metabolites identified following incubation of **1** with rat liver microsomes and NADPH/H^+.

In a broad screening, the interaction of the spiropiperidine **1** with more than 60 neurotransmitter receptors, ion channels, and neurotransmitter transporters was investigated in radioligand competition assays. The receptor systems included several adenosine, noradrenaline, dopamine, GABA, glutamate, histamine, muscarinic, nicotinic, opioid, purine and serotonin receptors. Various calcium, sodium and potassium channels, as well as transporters for dopamine, GABA, noradrenaline and serotonin, were also studied. At a test concentration of 1 μM, the spiropiperidine **1** did not compete significantly with the radioligands for these target systems. Moderate displacement of the radioligand [^{3}H]-ifenprodil from σ_2 receptors and a strong inhibition of [^{3}H]-haloperidol binding at σ_1 receptors was recorded.

In addition to this screening, the affinity of the spiropiperidine **1** to 5-HT_6 and 5-HT_7 receptors was investigated. At a concentration of 0.1 μM only a low level of displacement of the radioligands was observed.

In conclusion, the spiropiperidine **1** interacts with low nanomolar affinity (K_i 1.14 nM) with σ_1 receptors and shows an extraordinarily high selectivity for this receptor relative to the σ_2 receptor and more than 60 other neurotransmitter systems, ion channels and transporters.

Reaction with the hERG channel

The hERG channel is a voltage-gated potassium ion channel in the heart, blockade of which prolongs the QT interval in the electrocardiogram. Drugs that block the hERG channel increase the probability of ventricular arrhythmia, which may degenerate into ventricular fibrillation and cause sudden death.[34] Therefore, any potential interaction with the hERG channel is considered early during the development of a novel drug candidate.

CHO cells stably transfected with the hERG channel were used in the assay, which is based on the observation that the blockade of potassium channel activity is correlated to a positive shift in membrane potential, which can be measured by potentiometric dyes.[35,36]

The spiropiperidine **1** had little effect on the fluorescence intensity in this assay: about 92% of the hERG channel activity remained after incubation with 10 μM test compound **1**. Compared with the prototypical hERG channel blocker

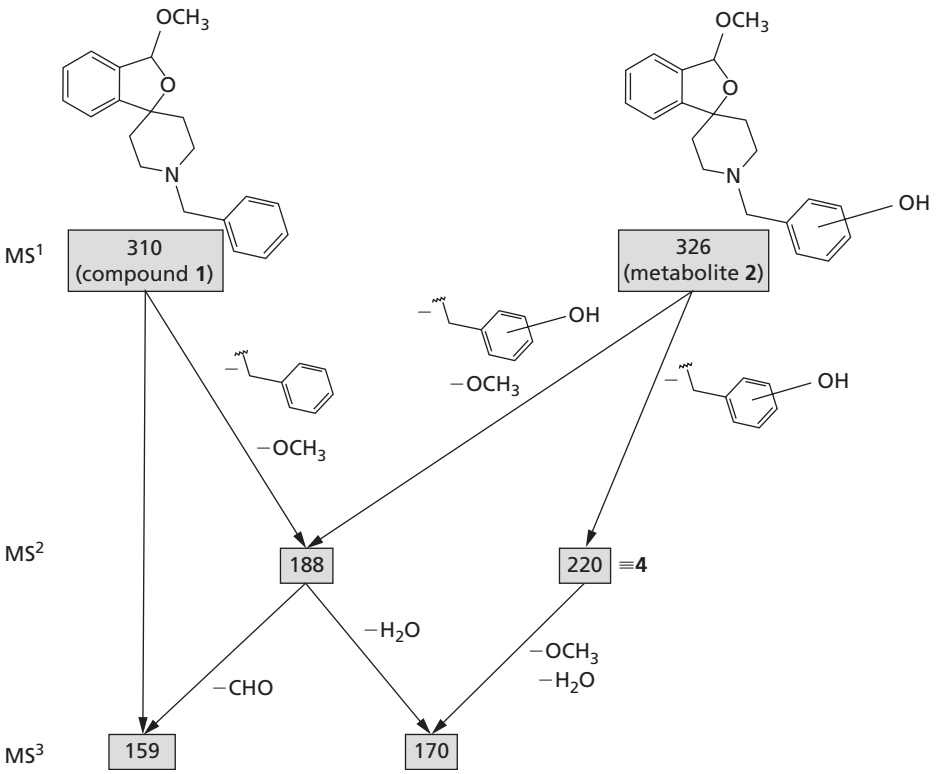

Figure 7 MS–MS–MS fragmentation pattern of the N-(hydroxybenzyl) metabolite **2**.

E-4031, which has an IC50 value of 12.3 nM in this assay, the hERG channel blocking activity of **1** is negligible. Thus it is highly unlikely that compound **1** will interact with this potassium channel to cause prolongation of the QT interval.

Analgesic activity

Subplantar capsaicin injection initially evokes a nocifensive behaviour that is characterised by lifting and guarding of the injected paw, which typically lasts up to 5 min after injection, after which hypersensitivity towards both thermal and mechanical stimuli is seen.[27] In this study, sensitisation by subplantar capsaicin injection was used to assess the effect of σ_1 ligands on mechanical allodynia.

Mice were treated with σ_1 ligands 30 min before capsaicin injection into the mid-plantar surface of the right hind paw and withdrawal latency to a mechanical stimulus by a von Frey filament determined 15 min after capsaicin injection. At a dose of 32 mg/kg, the spirocyclic piperidine **1** led to 88 ± 7.0% analgesia; a dose of 16 mg/kg still provided 53% ± 6.5% analgesia. For comparison, the IC50 value of the typical σ_1 receptor antagonist BD1063 was 16.1 ± 0.8 mg/kg after intraperitoneal injection.[30] Although an exact IC50 value for the spirocyclic piperidine **1** has not been reported, the data indicate that compound **1** has comparable analgesic activity to BD1063, indicating that it also is a σ_1 receptor antagonist.

We also gave the spirocyclic piperidine **1** to mice with partial sciatic nerve ligation. It did not elicit analgesic effects on nerve-injury-induced thermal hyperalgesia or mechanical allodynia at doses of 16, 32 or 64 mg/kg. A clear behavioural impairment was observed at a dose of 64 mg/kg, which lasted for only 5 min after administration, indicating very good tolerability of **1**.

In conclusion, the spirocyclic piperidine **1** shows considerable analgesic activity in the mouse capsaicin assay, indicating antiallodynic potency, which can be exploited for the treatment of mechanical allodynia.

Metabolism

The metabolic stability of the spirocyclic piperidine **1** was investigated in order to help the development of novel analgesics and PET ligands based on this compound. Both rat and human microsomes extensively metabolised compound **1**.

Identification of the formed metabolites is useful in the design of metabolically more stable σ_1 ligands. For this purpose the spirocyclic piperidine **1** was incubated with rat liver microsomes. An HPLC–UV method was developed to identify the parent compound **1** in the complex microsomal matrix (Figure 2). The degradation of the spirocyclic compound **1** during the incubation process is shown in Figure 3. After 30 min' incubation only 32% of the parent compound **1** remained, and only 10% after 60 min. These data reflect fast metabolic degradation of **1**.

The same HPLC method was then used to separate the formed metabolites (Figure 4). In order to get structural information about the metabolites, the separation method was transferred to an HPLC–MS system (Figure 5) equipped with a linear ion trap for fragmentation experiments. MS^n experiments combined with spiking of the samples with reference compounds[32,33] of potential metabolites led to the

identification of seven metabolites **2**–**8**, which are marked on the chromatograms. The structures of the identified metabolites are shown in Figure 6.

The major product was the secondary amine **4**, which was formed by N-debenzylation. The removal of the N-benzyl group was explained according to the established mechanism[38] of hydroxylation at the benzylic position to afford an unstable hemiaminal, which decomposes spontaneously to give the secondary amine **4** and benzaldehyde. Thus, modification of the N-benzyl residue should be considered in order to develop spirocyclic σ_1 ligands that are metabolically more stable. Further metabolites were formed by O-demethylation of the methoxy group (or hydrolysis of the acetal) to give the hemiacetal **5**, which reacted upon oxidation to the lactone **8**. Subsequent N-debenzylation and O-demethylation (or acetal hydrolysis) led to the very polar metabolite **7**.

In addition to the secondary amine **4,** the hydroxylated derivative **2** was also a main metabolite. Although the position of the hydroxy group at the phenyl moiety was not determined unequivocally by MS, we assume that the hydroxylation had taken place in the most active and easily accessible *p* position.

The fragmentation patterns of the parent compound **1** and the metabolite **2** are very similar (see Figure 7). Both compounds formed the peak at *m/z* 188, which was caused by the loss of the methoxy and the (substituted) benzyl moiety from parent compound **1** (–31 (OCH_3) –91 ($CH_2C_6H_5$)) or metabolite **2** (–31 (OCH_3) –107 ($CH_2C_6H_4OH$)). The fragment ion with *m/z* 188 was further decomposed to give a fragment with *m/z* 170 (loss of H_2O). The mass spectrum of metabolite **2** shows a further fragment at *m/z* 220, which corresponds to the secondary amine **4**. In the next fragmentation cycle (MS^3), the cation with *m/z* 170 was formed. Altogether, the loss of a hydroxylated benzyl moiety (M – 106) indicates clearly the hydroxylation at the N-benzyl moiety, excluding hydroxylation of the benzofuran substructure.

Only a very small amount of the N-oxide **3** was formed, which was even more lipophilic in the reversed-phase HPLC than the parent compound **1**. The structure of **3** could not be identified unequivocally by fragmentation experiments. Therefore, a substantial amount of **3** was required for NMR studies. Artificial oxidation systems can be used to produce this metabolite on a large scale. Oxidation of **1** with hydrogen peroxide led to a fast decomposition of the starting material but did not form the desired lipophilic N-oxide **3**. A system consisting of rat liver microsomes and different oxidation agents such as cumene hydroperoxide, *tert*-butyl hydroperoxide, hydrogen peroxide or $NaIO_4$ was therefore used. The combination of rat liver microsomes with hydrogen peroxide produced the N-oxide **3** in considerable amounts. The catalase activity of the microsome preparation led to formation of remarkable amounts of foam after addition of hydrogen peroxide, which complicated the transformation as well as the extraction and analysis of the formed metabolites. HPLC analysis showed two very similar products, representing the diastereomeric N-oxides **3**. The major N-oxide was purified by preparative HPLC and about 1 mg of the N-oxide **3** was isolated. The structure of the N-oxide **3** was confirmed unequivocally by ^{1}H NMR spectroscopy. A ^{1}H TOCSY experiment was performed to identify the signals of the piperidine protons, which proved the piperidinium substructure of **3**. In particular, the signals around the protons next to the piperidine-N-oxide are downfield shifted from 2.50 ppm ($N(CH_2CH_2)_2$), 2.84–2.89 ppm ($N(CH_2CH_2)_2$) and 3.60 ppm (NCH_2Ph) in **1** to 3.22–3.25 ppm ($N(CH_2CH_2)_2$), 3.57–3.64 ppm ($N(CH_2CH_2)_2$) and 4.47 ppm (NCH_2Ph) in **3**.

A second N-oxide **6** was observed during the HPLC analysis (see Figures 4 and 5), which was formed by oxidation of the hemiacetal **5** or O-demethylation (hydrolysis) of the N-oxide **3**. The fragmentation pattern in MS was similar to that of the N-oxide **3**.

The metabolism of compound **1** was also investigated using pooled human liver microsomes. The metabolic profile was similar to that obtained with rat liver microsomes but considerably less N-oxide **3** was formed and the second N-oxide **6** was not detected.

In order to elucidate which CYP enzymes are responsible for the fast degradation, the spirocyclic piperidine **1** was incubated with seven recombinant CYP450 isoenzymes (CYP1A2, CYP2B6, CYP2C8, CYP2C9, CYP2C19, CYP2D6 and CYP3A4) and the metabolites formed analysed using the established HPLC method. CYP3A4 produced all the identified metabolites, particularly the secondary amine **4** and the lactone **8**. Most of the physiologically relevant isoenzymes (CYP2B6, CYP2C8, CYP2C19 and CYP3A4) led to the formation of the hemiacetal **5**. CYP2C19 was predominantly responsible for the hydroxylation of the N-benzyl moiety, yielding the hydroxybenzyl metabolite **2**.

CYP2D6 did not produce metabolites to a large extent but the spirocyclic piperidine **1** had a high affinity for this enzyme (IC50 88 nM). Thus, the spirocyclic piperidine **1** is likely to be a potent inhibitor of CYP2D6. This inhibition of CYP2D6 needs to be eliminated from novel analgesics derived from the spirocyclic piperidine structure.

In conclusion, seven metabolites of the spirocyclic piperidine **1** were unequivocally identified after incubation with rat liver microsomes and the pattern of metabolites produced was similar in human microsomes. This knowledge about the structure of the metabolites will be helpful for the design of metabolically more stable PET tracers and analgesic drugs.

Conclusions

The spirocyclic piperidine **1** is a very potent and selective σ_1 receptor ligand. The analgesic activity in the capsaicin assay indicates that it is a σ_1 receptor antagonist. Incubation of **1** with rat liver microsomes resulted in rapid biotransformation. **1** is a potent inhibitor, but not a substrate, of CYP2D6. The strong inhibition of the isoenzyme CYP2D6 together with the rapid metabolism are disadvantages for the further development of **1** as an analgesic. However, the identification of the metabolites formed will allow the stabilisation of **1** with respect to metabolic degradation.

Declarations

Conflict of interest

The Author(s) declare(s) that they have no conflicts of interest to disclose.

Funding

This work was performed within the International Research Training Group 'Complex Functional Systems in Chemistry: Design, Synthesis and Applications' in collaboration with the University of Nagoya. Financial support of the IRTG and this project by the Deutsche Forschungsgemeinschaft is gratefully acknowledged. The experiments with the human microsomes and the recombinant isoenzymes were supported by Bayer HealthCare AG, Wuppertal, Germany.

References

1. Martin WR *et al*. The effects of morphine- and nalorphine-like drugs in the nondependent and morphine-dependent chronic spinal dog. *J Pharmacol Exp Ther* 1976; 197: 517–532.
2. Tam SW. Naloxone-inaccessible sigma receptor in rat central nervous system. *Proc Natl Acad Sci USA* 1983; 80: 6703–6707.
3. Gundlach AL *et al*. Phencyclidine and σ opiate receptors in brain: biochemical and autoradiographical differentiation. *Eur J Pharmacol* 1985; 113: 465–466.
4. Kaiser C *et al*. Sigma receptor ligands: function and activity. *Neurotransmission* 1991; 7: 1–5.
5. Walker JM *et al*. Sigma receptors: biology and function. *Pharmacol Rev* 1990; 42: 353–402.
6. Danso-Danquah R *et al*. Synthesis and σ binding properties of 2′-substituted 5,9α-dimethyl-6,7-benzomorphans. *J Med Chem* 1995; 38: 2978–2985.
7. Hanner M *et al*. Purification, molecular cloning, and expression of the mammalian sigma$_1$-binding site. *Proc Natl Acad Sci USA* 1996; 93: 8072–8077.
8. Seth P *et al*. Cloning and functional characterization of a receptor from rat brain. *J Neurochem* 1998; 70: 922–932.
9. Kekuda R *et al*. Cloning and functional expression of the human type 1 sigma receptor (hSigmaR1). *Biochem Biophys Res Comm* 1996; 229: 553–558.
10. Aydar E *et al*. The sigma receptor as a ligand regulated auxiliary potassium channel subunit. *Neuron* 2002; 34: 399–410.
11. Hellewell SB *et al*. Rat liver and kidney contain high densities of σ-1 and σ-2 receptors: characterization by ligand binding and photoaffinity labeling. *Eur J Pharmacol* 1994; 268: 9–18.
12. Hong W *et al*. Modulation of bradykinin-induced calcium changes in SH-SY5Y cells by neurosteroids and sigma receptor ligands via a shared mechanism. *Synapse* 2004; 54: 102–110.
13. Bermack JE, Debonnel G. Distinct modulatory roles of sigma receptor subtypes on glutamatergic responses in the dorsal hippocampus. *Synapse* 2005; 55: 37–44.
14. Gudelsky GA. Biphasic effect of sigma receptor ligands on the extracellular concentration of dopamine in the striatum of the rat. *J Neural Transm* 1999; 106: 849–856.
15. Bowen WD. Sigma receptors: recent advances and new clinical potentials. *Pharm Acta Helv* 2000; 74: 211–218.
16. Wilke RA *et al*. K^+ channel modulation in rodent neurohypophysial nerve terminals by sigma receptors and not by dopamine receptors. *J Physiol* 1999; 517: 391–406.
17. Aydar E *et al*. Sigma receptors and cancer: possible involvement of ion channels. *Cancer Res* 2004; 64: 5029–5035.
18. Monnet FP. Sigma-1 receptor as regulator of neuronal intracellular Ca^{2+}: clinical and therapeutic relevance. *Biol Cell* 2005; 97: 873–883.
19. Zhang H, Cuevas J. Sigma receptors inhibit high-voltage–activated calcium channels in rat sympathetic and parasympathetic neurons. *J Neurophysiol* 2002; 87: 2867–2879.
20. Rowley M *et al*. Current and novel approaches to the drug treatment of schizophrenia. *J Med Chem* 2001; 44: 477–501.
21. Anon. Monograph igmesine hydrochloride. *Drugs Fut* 1999; 24: 133–140.
22. Skuza G. Potential anidepressant activity of sigma ligands. *Pol J Pharmacol* 2003; 55: 923–934.
23. Maurice T, Lockhart BP. Neuroprotective and anti-amnesic potentials of σ (sigma) receptor ligands. *Prog Neuropsychopharmacol Biol Psychiatry* 1997; 21: 69–102.
24. Marrazzo A *et al*. Neuroprotective effects of sigma-1 receptor agonists against beta-amyloid-induced toxicity. *Neuroreport* 2005; 18: 1223–1226.
25. Matsumotoa RR *et al*. σ-Receptors: potential medications development target for anti-cocaine agents. *Eur J Pharmacol* 2003; 496: 1–12.
26. Hayashi T, Su T-P. σ_1 receptor ligands: potential in the treatment of neuropsychiatric disorders. *CNS Drugs* 2004; 18: 269–284.
27. Gilchrist HD *et al*. Enhanced withdrawal responses to heat and mechanical stimuli following intraplantar injection of capsaicin in rats. *Pain* 1996; 67: 179–188.
28. Baeyens JM. Use of compounds active at the sigma receptor for the treatment of allodynia. *PCT Int Appl* WO 2006/010587 A1 2006.
29. Kim KW *et al*. Selective sigma-1 receptor antagonist produces antinociceptive effect in neuropathic pain models in rats. *FASEB J* 2008; 22: lb618.
30. Entrena JM *et al*. Sigma-1 receptor agonists sensitize mice to capsaicin-induced mechanical allodynia. *Behav Pharmacol* 2005; 16(Suppl. 1): S107.
31. Langa F *et al*. Generation and phenotypic analysis of sigma receptor type 1 (σ1) knockout mice. *Eur J Neurosci* 2003; 18: 2188–2196.
32. Maier CA, Wünsch B. Novel spiropiperidines as highly potent and subtype selective σ-receptor ligands. Part 1. *J Med Chem* 2002; 45: 438–448.
33. Maier CA, Wünsch B. Novel σ receptor ligands. Part 2. SAR of spiro[[2]benzopyran-1,4′-piperidines] and spiro[[2]benzofuran-1,4′-piperidines] with carbon substituents in position 3. *J Med Chem* 2002; 45: 4923–4930.
34. Recanatini M *et al*. QT prolongation through hERG K^+ channel blockade: current knowledge and strategies for the early prediction during drug development. *Med Res Rev* 2005; 25: 133–166.
35. Plásek J, Sigler K. Slow fluorescent indicators of membrane potential: a survey of different approaches to probe response analysis. *J Photochem Photobiol* 1996; 33: 101–124.
36. Warnke JW, Ganetzky B. A family of potassium channel genes related to eag in Drosophila and mammals. *Proc Nat Acad Sci USA* 1994; 91: 3438–3442.
37. Dayer P, Gasser R. Characterization of a common genetic defect of cytochrome P-450 function. *Biochem Biophys Res Commun* 1984; 30: 374–380.
38. Testa B, Jenner P. *Drug Metabolism: Chemical and Biochemical Aspects.* Drugs and the Pharmaceutical Sciences Series, vol. 4, Swarbrick J, ed. New York: Marcel Dekker, 1976: 82.